

Developmental Cell

Molecular Pathway of Microtubule Organization at the Golgi Apparatus

Highlights

- CAMSAP2 stabilizes microtubule minus ends at the Golgi
- A complex of AKAP450 and myomegalin recruits CAMSAP2-bound microtubules to the Golgi
- A single Golgi can be maintained in the absence of centrosome and Golgi microtubules
- Golgi microtubules facilitate cell reorientation and migration in 3D matrix

Authors

Jingchao Wu, Cecilia de Heus, Qingyang Liu, ..., Robert Z. Qi, Judith Klumperman, Anna Akhmanova

Correspondence

a.akhmanova@uu.nl

In Brief

Wu et al. describe how a microtubule minus-end-binding protein, CAMSAP2, acts together with Golgi-associated proteins AKAP450 and myomegalin to promote microtubule organization at the Golgi. They also show how these proteins affect cell migration and describe the redundancy between the centrosome-dependent and -independent pathways in microtubule minus-end stabilization.



Molecular Pathway of Microtubule Organization at the Golgi Apparatus

Jingchao Wu,¹ Cecilia de Heus,² Qingyang Liu,¹ Benjamin P. Bouchet,¹ Ivar Noordstra,¹ Kai Jiang,¹ Shasha Hua,¹ Maud Martin,¹ Chao Yang,¹ Ilya Grigoriev,¹ Eugene A. Katrukha,¹ A.F. Maarten Altelaar,³ Casper C. Hoogenraad,¹ Robert Z. Qi,⁴ Judith Klumperman,² and Anna Akhmanova^{1,5,*}

¹Cell Biology, Department of Biology, Faculty of Science, Utrecht University, Padualaan 8, 3584 CH Utrecht, the Netherlands

²Department of Cell Biology, Center for Molecular Medicine, University Medical Center Utrecht, Heidelberglaan 100, 3584 CX Utrecht, the Netherlands

³Biomolecular Mass Spectrometry and Proteomics, Bijvoet Center for Biomolecular Research, Utrecht Institute for Pharmaceutical Sciences, The Netherlands Proteomics Centre, Utrecht University, Padualaan 8, 3584 CH Utrecht, the Netherlands

⁴Division of Life Science, The Hong Kong University of Science and Technology, Clear Water Bay, Kowloon, Hong Kong, China

⁵Lead Contact

*Correspondence: a.akhmanova@uu.nl

<http://dx.doi.org/10.1016/j.devcel.2016.08.009>

SUMMARY

The Golgi apparatus controls the formation of non-centrosomal microtubule arrays important for Golgi organization, polarized transport, cell motility, and cell differentiation. Here, we show that CAMSAP2 stabilizes and attaches microtubule minus ends to the Golgi through a complex of AKAP450 and myomegalin. CLASPs stabilize CAMSAP2-decorated microtubules but are not required for their Golgi tethering. AKAP450 is also essential for Golgi microtubule nucleation, and myomegalin and CDK5RAP2 but not CAMSAP2 contribute to this function. In the absence of centrosomes, AKAP450- and CAMSAP2-dependent pathways of microtubule minus-end organization become dominant, and the presence of at least one of them is needed to maintain microtubule density. Strikingly, a compact Golgi can be assembled in the absence of both centrosomal and Golgi microtubules. However, CAMSAP2- and AKAP450-dependent Golgi microtubules facilitate Golgi reorientation and cell invasion in a 3D matrix. We propose that Golgi-anchored microtubules are important for polarized cell movement but not for coalescence of Golgi membranes.

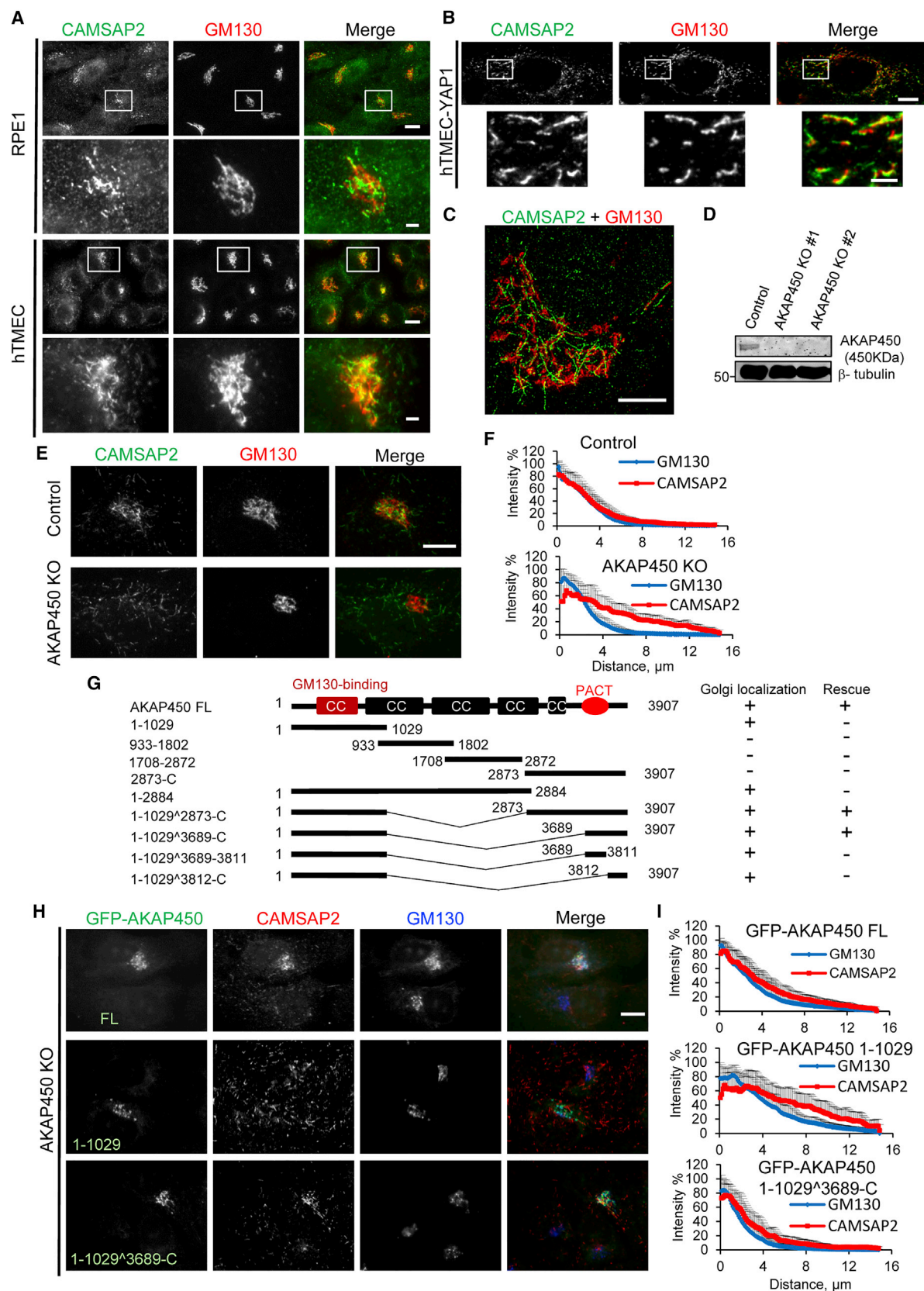
INTRODUCTION

Microtubule (MT) organization is governed by MT-organizing centers (MTOCs), the sites responsible for MT nucleation as well as stabilization and attachment of MT minus ends. In many types of cultured mammalian cells, the centrosome serves as a dominant MTOC (Conduit et al., 2015). However, even in cells with a radial MT organization, a significant proportion of the MT minus ends is not attached to the centrosome (Akhmanova and Hoogenraad, 2015). In recent years, the Golgi apparatus has emerged as a site that can nucleate and stabilize MTs (Chabin-Brion et al., 2001; Rios, 2014; Sanders and Kaver-

ina, 2015; Zhu and Kaverina, 2013). Golgi-derived MTs participate in Golgi reassembly after cell division by promoting fusion of the Golgi stacks into the Golgi ribbon (Nakamura et al., 2012; Rios, 2014; Zhu and Kaverina, 2013). Furthermore, unlike centrosomal MTs, Golgi-anchored MT arrays are polarized and can thus promote cell asymmetry and polarized transport of post-Golgi carriers that are important for cell migration (Hurtado et al., 2011; Vinogradova et al., 2009, 2012). Finally, in differentiated cell types, such as muscle cells, pancreatic β cells, and neurons, Golgi membranes can serve as MTOCs controlling the formation of non-centrosomal MT arrays, which are required for cell morphogenesis and function, such as neurite outgrowth and branching in neuronal cells (Oddoux et al., 2013; Ori-McKenney et al., 2012; Yalgin et al., 2015; Zhu et al., 2015).

Several factors have been shown to be required for the formation of Golgi-anchored MT arrays. AKAP450 (A-kinase anchoring protein of 450 kDa, also known as AKAP350, AKAP9, or CG-NAP) (Schmidt et al., 1999; Takahashi et al., 1999; Witczak et al., 1999) is a large centrosomal and Golgi protein, which is recruited to the *cis* Golgi by the Golgi matrix protein GM130 (Hurtado et al., 2011). AKAP450 is required for MT nucleation from the Golgi (Rivero et al., 2009). This function might depend on the association of the N terminus of AKAP450 with γ -tubulin ring complex (γ -TURC) (Takahashi et al., 2002), although this interaction was disputed (Hurtado et al., 2011). AKAP450 can also recruit to the Golgi two γ -TURC-binding homologous proteins, CDK5RAP2 (also known as CEP215) and myomegalin (MMG) (Choi et al., 2010; Roubin et al., 2013; Wang et al., 2010, 2014). The *Drosophila* homologs of AKAP450 and CDK5RAP2, CP309 and centrosomin, control MT outgrowth from Golgi outposts in fly neurons (Ori-McKenney et al., 2012; Yalgin et al., 2015).

Another line of research showed that CLASPs, which are recruited to *trans* Golgi by the golgin GCC185, are also necessary for the nucleation and organization of Golgi-anchored MTs (Efimov et al., 2007; Miller et al., 2009). CLASPs are MT plus-end tracking proteins (+TIPs), which can stabilize MTs and promote rescues (Mimori-Kiyosue et al., 2005). Furthermore, both AKAP450 and CLASPs can interact with the MT lattice-binding protein MTCL1, which enhances MT association with the Golgi (Sato et al., 2014).



(legend on next page)

The emerging picture of the Golgi-dependent MT organization is thus complex, as it involves tethering of MT-nucleating and -stabilizing proteins at both *cis* and *trans* Golgi, and it is currently unclear how these proteins work together in the same pathway. It is also unclear whether these proteins are sufficient for not only nucleating but also stabilizing MT minus ends that are not attached to the centrosome. Recent work has identified the members of the calmodulin-regulated spectrin-associated (CAMSAP)/Patronin/Nezha family as factors crucial for stabilizing non-centrosomal MT minus ends in different settings (Akhmanova and Hoogenraad, 2015). In mammalian cells, CAMSAP2 and CAMSAP3 were shown to recognize and decorate growing MT minus ends and thus form MT minus-end associated stretches of $\sim 1\text{--}2\text{ }\mu\text{m}$ in length that prevent MT depolymerization and serve as a source of MT plus-end outgrowth (Jiang et al., 2014; Tanaka et al., 2012). Importantly, it was shown that in human retinal pigment epithelium (RPE1) cells, which are often used as a model to study Golgi-anchored MTs, CAMSAP2 depletion leads to the loss of most non-centrosomal MTs (Jiang et al., 2014), suggesting that CAMSAP2 participates in MT stabilization at the Golgi.

Here, we found that CAMSAP2 is essential for the tethering, but not for nucleation of non-centrosomal MTs at the Golgi. Using CRISPR/Cas9 knockout (KO) and rescue experiments, we showed that CAMSAP2 localization to the Golgi depends on a complex of AKAP450 and MMG. CLASPs are not required for the binding of CAMSAP2-decorated MT stretches to the Golgi but rather promote their stability. AKAP450, but not MMG or CDK5RAP2, is essential for MT nucleation from the Golgi when cells recover from MT disassembly. AKAP450 thus has a dual function in organizing Golgi MTs, by tethering CAMSAP2-bound MT minus ends and by promoting MT nucleation through γ -TURC recruitment.

We next explored the redundancy between different MT nucleation and minus-end stabilization pathways by depleting centrioles in different KO lines using Plk4 inhibitor centrinone (Wong et al., 2015). We found that in the absence of centrosomes, AKAP450 and MMG enhanced the interaction of γ -tubulin and MTs with the Golgi membranes. In cells lacking centrosomes as well as AKAP450 or MMG, MT abundance in the Golgi area was dramatically reduced, but the Golgi was still highly compact. Electron microscopy (EM) revealed no differences in the morphology of individual Golgi stacks in cells simultaneously depleted of AKAP450 and centrosomes, but showed that more

vesicles were present in the Golgi area, suggesting that vesicular trafficking but not the coalescence of the Golgi membranes requires abundant Golgi-associated MTs. When both CAMSAP2 and AKAP450 were removed, the majority of cells that survived after centriole depletion had a radial MT network anchored at a single, strongly enlarged acentriolar MTOC, which contained centrosomal markers. This suggests that clustering of centrosomal proteins in a single MTOC becomes more critical for cell survival when non-centrosomal MT minus-end stabilization pathways are disabled. Finally, we found that the loss of Golgi-anchored MTs affected the ability of the Golgi to reorganize rapidly in migrating cells and the ability of cancer cells to invade collagen matrix. Taken together, our data show how different MT- and Golgi-bound factors work together to control Golgi-anchored MTs, and demonstrate the importance of Golgi-attached MTs for the architecture of acentrosomal cells and for cell motility.

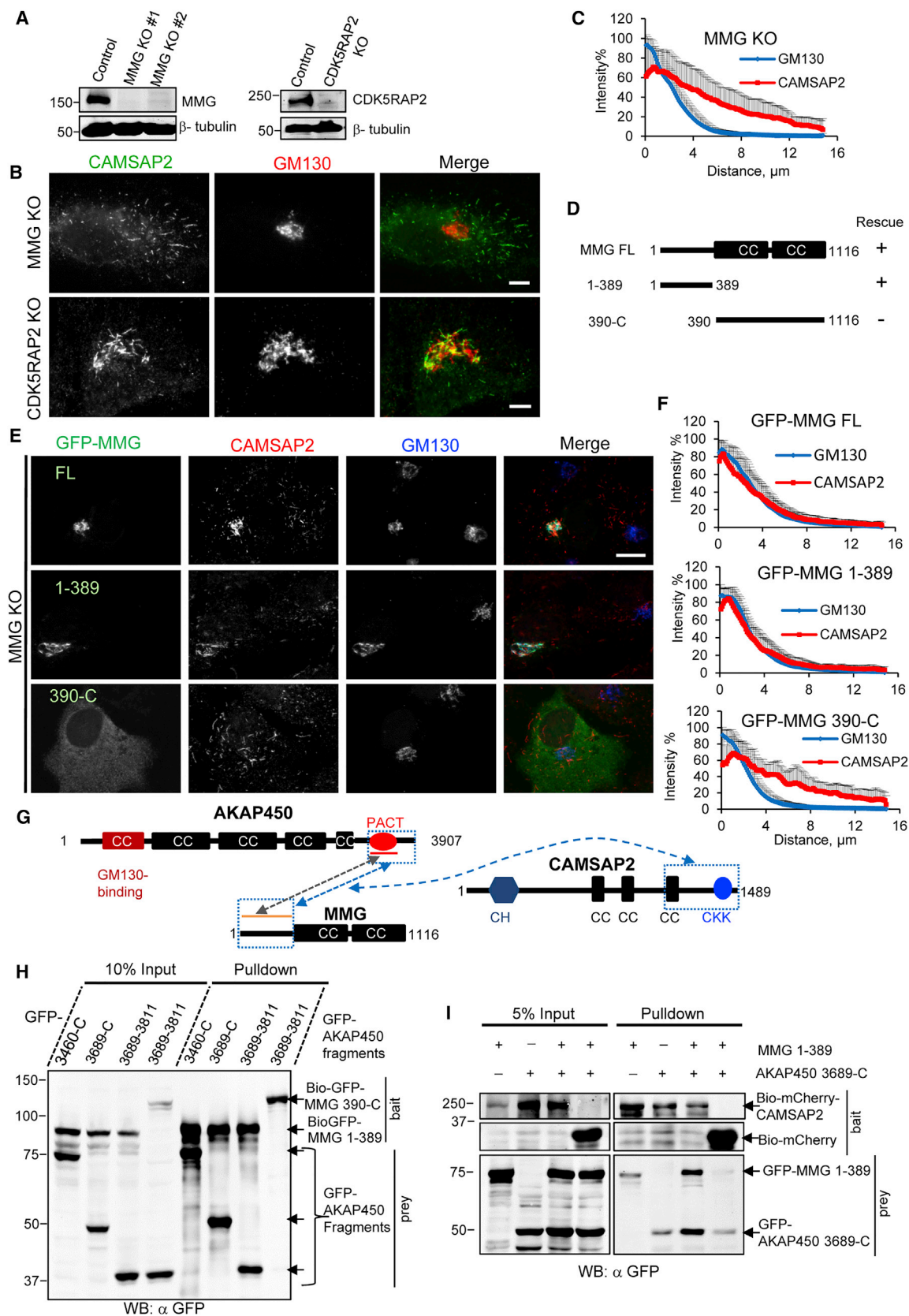
RESULTS

CAMSAP2-Decorated MT Minus Ends Associate with the Golgi in an AKAP450-Dependent Manner

To understand how non-centrosomal MT minus ends are organized, we first investigated the localization of CAMSAP2-stabilized MTs in different cell lines. Prominent co-localization of CAMSAP2 stretches with the Golgi, but not with lysosomes or endosomes, was observed in cells with relatively sparse MT systems, such as RPE1, hTERT-immortalized human mammary epithelial cells (hTMECs), and human umbilical vein endothelial cells (Figures 1A, S1A, and S1B), as well as fibrosarcoma HT1080 cells (see below), which all lack detectable CAMSAP3 expression (data not shown). The specificity of CAMSAP2-Golgi co-localization was confirmed in an hTMEC cell line, which was converted to a mesenchymal phenotype by expressing transcription factor YAP1 (Overholtzer et al., 2006) and exhibited strongly dispersed Golgi stacks (Figure 1B). Furthermore, super-resolution microscopy showed that CAMSAP2 stretches could fully co-align or partially overlap with individual Golgi stacks (Figure 1C). Co-localization between CAMSAP2 and the Golgi was less apparent in cells that have dense non-centrosomal MT arrays and express CAMSAP3, such as HeLa or Caco-2 (Nagae et al., 2013; Toya et al., 2016) (data not shown), likely due to the recruitment of MT minus ends to other sites such as the cell cortex.

Figure 1. CAMSAP2-Decorated MT Stretches Localize to the Golgi in AKAP450-Dependent Manner

- (A) Immunostaining of CAMSAP2 (green) and GM130 (red) in RPE1 and hTMEC. Scale bars, 10 μm ; in the enlargements, 2 μm .
 (B) Immunostaining of CAMSAP2 (green) and GM130 (red) in hTMEC cells after the induction of YAP1 expression with 1 $\mu\text{g}/\text{mL}$ doxycycline for 3 days. Scale bars, 10 μm ; in the enlargements, 2 μm .
 (C) Structured illumination microscopy image of the immunostaining of CAMSAP2 (green) and GM130 (red) in RPE1 cells. Scale bar, 5 μm .
 (D) Western blot of extracts of RPE1 cells prepared from control and AKAP450 KO lines.
 (E) Immunostaining of CAMSAP2 (green) and GM130 (red) in control or AKAP450 KO cells. Scale bar, 10 μm .
 (F) Quantification CAMSAP2 and GM130 distribution in control/AKAP450 KO cells. Distance from the center of the Golgi is shown on the horizontal axis and normalized fluorescence intensity on the vertical axis. Thirty-five cells were analyzed per condition. Error bars represent SD.
 (G) Domain organization of AKAP450 and the deletion mutants used to rescue CAMSAP2 localization at the Golgi. PACT, pericentrin-AKAP450 centrosomal targeting domain; CC, coiled coil. Golgi localization and rescue of CAMSAP2 accumulation at the Golgi are indicated.
 (H) Immunostaining of CAMSAP2 (red) and GM130 (blue) in AKAP450 KO cells overexpressing GFP-tagged full-length (FL) AKAP450 or the indicated AKAP450 mutants (green). Scale bar, 10 μm .
 (I) Quantification of CAMSAP2 and GM130 distribution in cells shown in (G), analyzed and displayed as in (F).
 See also Figure S1, Table S1, and Movies S1 and S2.



(legend on next page)

To investigate how CAMSAP2 stretches attach to the Golgi, we performed streptavidin pull-down assays with biotinylation (Bio)-tagged CAMSAP2 (Jiang et al., 2014), analyzed the precipitated proteins by mass spectrometry, and identified AKAP450 as one of the potential partners (Table S1). Transient depletion of AKAP450 with small interfering RNAs (siRNAs) or permanent removal of AKAP450 by CRISPR/Cas9-mediated KO in RPE1 cells led to the detachment of CAMSAP2 stretches from the Golgi and their redistribution into the cytoplasm (Figures 1D–1F and S1C–S1E), while cell viability and proliferation were not significantly affected. The localization of CAMSAP2 stretches to the Golgi could be restored by expressing in AKAP450 KO cells the full-length GFP-AKAP450, but not the AKAP450 fragments, which localized either to the Golgi (the N-terminal part), cytosol (the middle parts of AKAP450) or the centrosome (the C-terminal part, containing the pericentrin-AKAP450 centrosomal targeting [PACT] domain) (Gillingham and Munro, 2000) (Figures 1G–1I and S1F). By making internal deletions, we have identified the minimal region of AKAP450, including the PACT domain and AKAP450 C terminus, required for the localization of CAMSAP2 stretches to the Golgi when fused to the Golgi-binding AKAP450 N terminus (Figures 1G–1I and S1F).

We then used cell recovery from the MT-depolymerizing drug nocodazole to observe how nascent CAMSAP2 stretches associate with the Golgi. As shown previously, CAMSAP2-decorated MTs emerged with a delay after MTs were formed at the centrosome, Golgi membranes, and other cytoplasmic sites (Jiang et al., 2014). Importantly, not only the CAMSAP2 stretches that appeared at the Golgi but also those formed near the centrosome could associate with the reassembling Golgi apparatus (Figure S1G and Movie S1). In contrast, no Golgi association of emerging CAMSAP2 stretches was observed in AKAP450 KO cells (Figure S1G and Movie S2). We conclude that CAMSAP2 stretches can be captured and laterally attached to the Golgi membranes, and that AKAP450 is required for this process.

MMG Is Required for the Binding of CAMSAP2-Decorated MTs to the Golgi

We next attempted to demonstrate an interaction between the AKAP450 C terminus and CAMSAP2 but detected only weak

binding (not shown). We then reasoned that additional factors might participate in this interaction and searched for them by pull-down assays combined with mass spectrometry using the C-terminal part of AKAP450 (amino acids 2,873–3,907). We identified several proteins, including MMG isoform 8 (hereafter called MMG) and CDK5RAP2 (Table S1), which were previously reported to bind to AKAP450 (Roubin et al., 2013; Wang et al., 2010, 2014). We have generated RPE1 KO lines lacking MMG or CDK5RAP2 (Figure 2A), which were both viable and displayed no strong cell-proliferation defects. We found that while CDK5RAP2 KO had no effect on CAMSAP2 localization, the loss of MMG resulted in the detachment of CAMSAP2 stretches from the Golgi (Figures 2B and 2C). Re-expression of the full-length MMG or its the N-terminal part (amino acids 1–389) restored the localization of CAMSAP2 stretches to the Golgi (Figures 2D–2F). Similar to previously published work (Wang et al., 2014), we found that the loss of MMG led to a decreased expression of AKAP450, which could be rescued by the expression of both the full-length MMG and its N-terminal part (Figures S2A–S2D). We also confirmed that the N terminus of MMG strongly bound to AKAP450, and deletion mapping showed that the PACT domain of AKAP450 was by itself sufficient for the binding to MMG N terminus (Figures 2G and 2H).

Importantly, while the AKAP450 C terminus and MMG N terminus displayed only weak binding to CAMSAP2 when they were expressed separately, a much better binding was observed when they were expressed together (Figure 2I). We next extended the pull-down assays to a series of CAMSAP2-deletion mutants and found that the complex of AKAP450 C terminus and MMG N terminus interacted with the C-terminal part of CAMSAP2 encompassing the last coiled coil and the CKK domain, the CAMSAP2 part previously shown to be required for MT minus-end decoration and stabilization (Jiang et al., 2014) (Figures 2G, S2E, and S2F). We conclude that CAMSAP2 binds to a complex formed by AKAP450 and MMG. We note that this interaction is rather weak compared with the strong interaction between AKAP450 and MMG. This fits well with the fact that we could detect no recruitment of soluble CAMSAP2 to the Golgi membranes in cells with disassembled MTs (Figure S1G and data not shown). CAMSAP2 recruitment to the Golgi thus occurs in the form of CAMSAP2-decorated MT stretches.

Figure 2. MMG Is Required for the Binding of CAMSAP2-Decorated MTs to the Golgi

(A) Western blots of extracts of RPE1 cell lines knocked out for MMG or CDK5RAP2.

(B) Immunostaining of CAMSAP2 (green) and GM130 (red) in MMG or CDK5RAP2 KO cells. Scale bar, 5 μ m.

(C) Quantification of CAMSAP2 and GM130 distribution in MMG KO cells, analyzed and displayed as in Figure 1F.

(D) Domain organization of MMG and the deletion mutants used to rescue CAMSAP2 localization at the Golgi. +, rescue; –, no rescue.

(E) Immunostaining of CAMSAP2 (red) and GM130 (blue) in MMG KO RPE1 cells overexpressing the indicated GFP-tagged MMG constructs (green). Scale bar, 10 μ m.

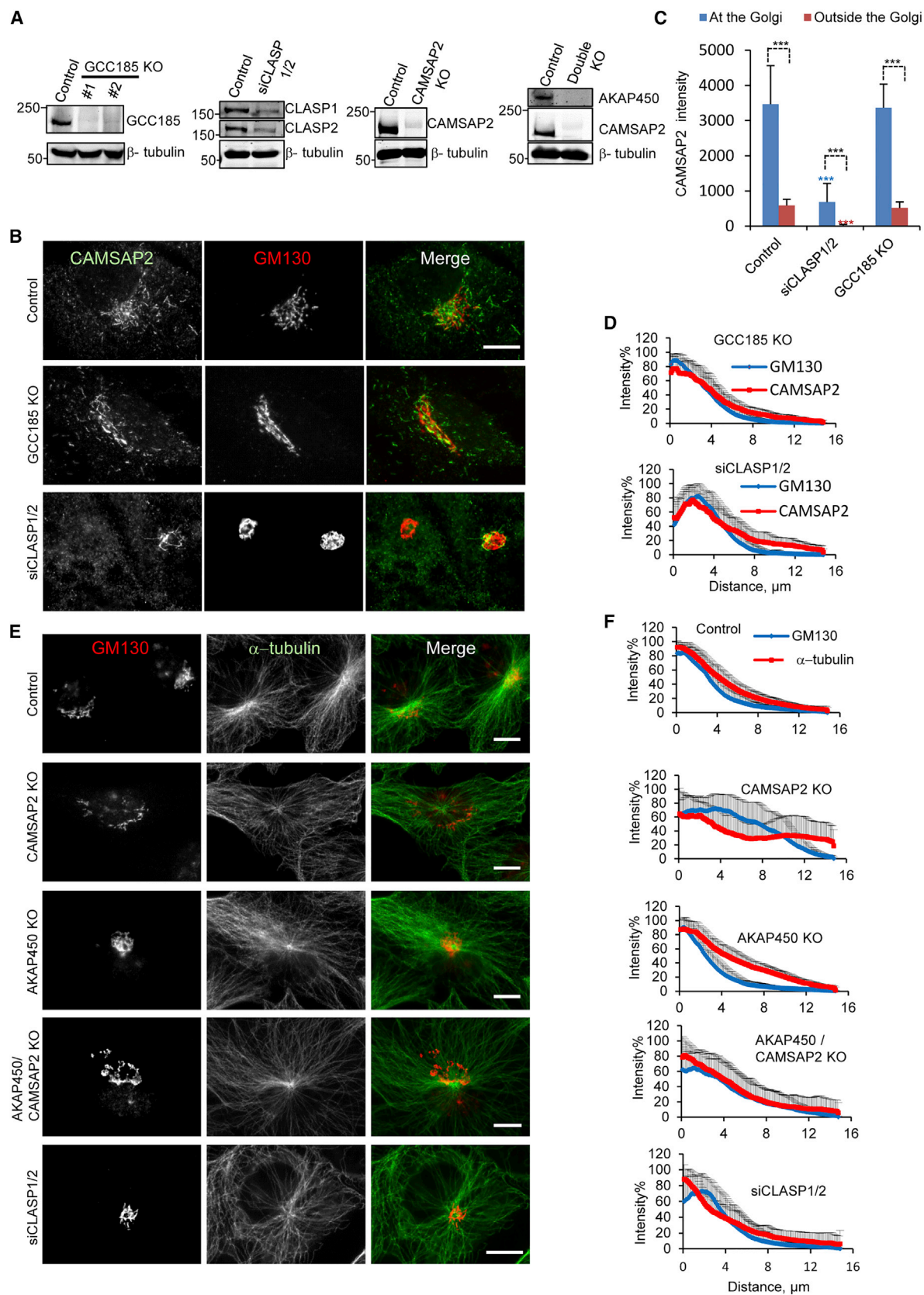
(F) Quantification of CAMSAP2 and GM130 distribution in cells shown in (E), analyzed and displayed as in Figure 1F.

(G) Schematic representation of the interactions between AKAP450, MMG, and CAMSAP2. CH, calponin homology domain; CKK, C-terminal domain common to CAMSAP1, KIAA1078, and KIAA1543; other abbreviations are the same as in Figure 1G. AKAP450 binds to MMG N terminus (1–389 binds) through its PACT domain (gray arrow), while a larger C-terminal fragment of AKAP450 in complex with MMG N terminus is needed for the interaction with CAMSAP2 C terminus (blue boxes and arrow).

(H) Streptavidin pull-down assays performed with the extracts of HEK293T cells co-expressing biotinylation and GFP (Bio-GFP) tagged MMG mutants 1–389 (first three lanes) or 390–1,116 (fourth lane), the indicated GFP-AKAP450 deletion mutants and BirA, and analyzed by western blotting (WB).

(I) Streptavidin pull-down assays performed with the extracts of HEK293T cells co-expressing Bio-mCherry-CAMSAP2 or Bio-mCherry, together with the indicated combinations of GFP-AKAP450 or GFP-MMG deletion mutants and BirA, and analyzed by western blotting with streptavidin IRDye 680RD (upper panels) or anti-GFP antibodies (lower panel).

See also Figure S2.



(legend on next page)

CLASPs Are Required for Stabilization but Not for Golgi Tethering of CAMSAP2-Bound MTs

We next set out to test the role of CLASPs, +TIPs important for controlling Golgi-derived MTs (Efimov et al., 2007), in the organization CAMSAP2-decorated MT minus ends. CLASPs are targeted to the *trans* Golgi by the golgin GCC185 (Efimov et al., 2007). We generated GCC185 KO RPE1 cells (Figure 3A) and found that CLASP2 was lost from the Golgi but not from the centrosome, as previously published, while CAMSAP2 stretches were retained at the Golgi (Figures 3B–3D, S3A, and S3B). Since CLASPs are essential for cell division, we could not generate double CLASP1/2 KO lines and resorted to siRNA-mediated protein depletion (Figure 3A). Simultaneous knockdown of CLASP1 and CLASP2 resulted in a strong reduction in the number or even complete loss of CAMSAP2 stretches both at the Golgi and in the cytoplasm (Figures 3B and 3C). However, in cells where some CAMSAP2 stretches were still present, they were tightly associated with the Golgi (Figures 3B–3D). We conclude that the Golgi-bound CLASP pool is not required for CAMSAP2 recruitment to the Golgi, but CLASPs can stabilize CAMSAP2 stretches throughout the cell.

MT and Golgi Organization in the Absence of Golgi-Anchored MTs

We next compared the effect of removal of different factors on Golgi-MT co-organization. Our previous work showed that siRNA-mediated depletion of CAMSAP2 leads to a dramatic loss of non-centrosomal MTs in RPE1 cells (Jiang et al., 2014). To confirm these results, we generated CAMSAP2 KO RPE1 cells (Figure 3A). These cells were viable and displayed no obvious defects in cell-cycle progression, in line with the fact that CAMSAP2 detaches from MTs during mitosis and does not participate in cell division (Jiang et al., 2014). Furthermore, in addition to single KOs we generated double-KO lines missing MMG and CDK5RAP2, or AKAP450 and CAMSAP2, a triple MMG, CDK5RAP2, and AKAP450 KO, and a quadruple-KO line lacking MMG, CDK5RAP2, AKAP450, and CAMSAP2 (Figures 3A and S3C). Also these lines could be successfully propagated, indicating that none of these proteins or their combinations is essential for RPE1 cell survival.

We found that in all cell lines lacking CAMSAP2, MT density in the Golgi area was strongly reduced, whereas the remaining MTs radiated from the centrosome (Figures 3E, 3F, S3D, and S3E). In contrast, in cell lines lacking AKAP450 or MMG but still expressing CAMSAP2 there was a significant proportion of non-centrosomal MTs detached from the Golgi area, in line with the presence of dispersed non-centrosomal CAMSAP2-decorated

MT minus ends (Figures 3E, 3F, S3D, and S3E). Some detachment of non-centrosomal MTs from the Golgi was also observed in the GCC185 KO line, although the effect was mild (Figures S3D and S3E). In CLASP-depleted cells, the MT system became more radial and the MT density around the Golgi was lost, consistent with the disappearance of CAMSAP2 stretches (Figures 3E and 3F).

In CAMSAP2 KO cells, separate Golgi stacks were located around the centrosome and their organization was less compact than in control cells (Figures 3E and 3F). In AKAP450 and MMG KO cells, the Golgi was strongly clustered around the centrosome, consistent with the previously published data on AKAP450 (Hurtado et al., 2011) (Figures 3E, 3F, S3D, and S3E). It is possible that CAMSAP2-stabilized non-centrosomal MTs can contribute to the compaction of Golgi membranes, even if they are not attached to them, by serving as tracks for their transport.

AKAP450 but Not CAMSAP2 Is Involved in MT Nucleation from the Golgi

Previous work has shown that AKAP450 plays a critical role in MT nucleation from the Golgi during recovery from MT disassembly (Hurtado et al., 2011; Rivero et al., 2009). However, it remained unclear whether it performs this function by recruiting MT-nucleating factors such as γ -TURC directly or through its binding partners CDK5RAP2 and MMG. Using the KO cell lines described above, we found that while the KO of CAMSAP2 or MMG had no effect on MT nucleation after nocodazole washout, MT nucleation from the Golgi membranes was reduced in CDK5RAP2 KO and an even stronger reduction was seen in the double CDK5RAP2/MMG KO (Figures 4A and 4B). A complete loss of MT nucleation from the Golgi was observed in all AKAP450 KO lines (Figures 4A and 4B). Importantly, re-expression in the triple AKAP450/CDK5RAP2/MMG KO cells of CDK5RAP2, but not MMG, increased MT nucleation in the cytoplasm, though not from the Golgi membranes, to which CDK5RAP2 could not be recruited in the absence of AKAP450 (Figure 4C). This result is consistent with the previous data showing that CDK5RAP2 can stimulate the MT-nucleating activity of γ -TURC (Choi et al., 2010).

MT nucleation from the Golgi could be partially restored in the triple AKAP450/CDK5RAP2/MMG KO cells by expressing the full-length AKAP450 (Figures 4B and 4D). The N-terminal part of AKAP450, which was previously reported to bind to γ -TURC (Takahashi et al., 2002), did not rescue MT nucleation from the Golgi (Figures 4B and 4D). However, we did observe rescue of MT nucleation from the Golgi membranes in cells expressing

Figure 3. The Role of CLASPs in Stabilization of CAMSAP2-Decorated MTs and the Effect of the Loss of Different Proteins on the Golgi and MT Organization

(A) Western blots of extracts of RPE1 cells cultured for 72 hr after the co-transfection with the siRNAs for CLASP1 and CLASP2 (second panel) or prepared from control or indicated KO lines (first, third, and fourth panels).

(B) Immunostaining of CAMSAP2 (green) and GM130 (red) in control, GCC185 KO, or CLASP1/2-depleted cells. Scale bar, 10 μ m.

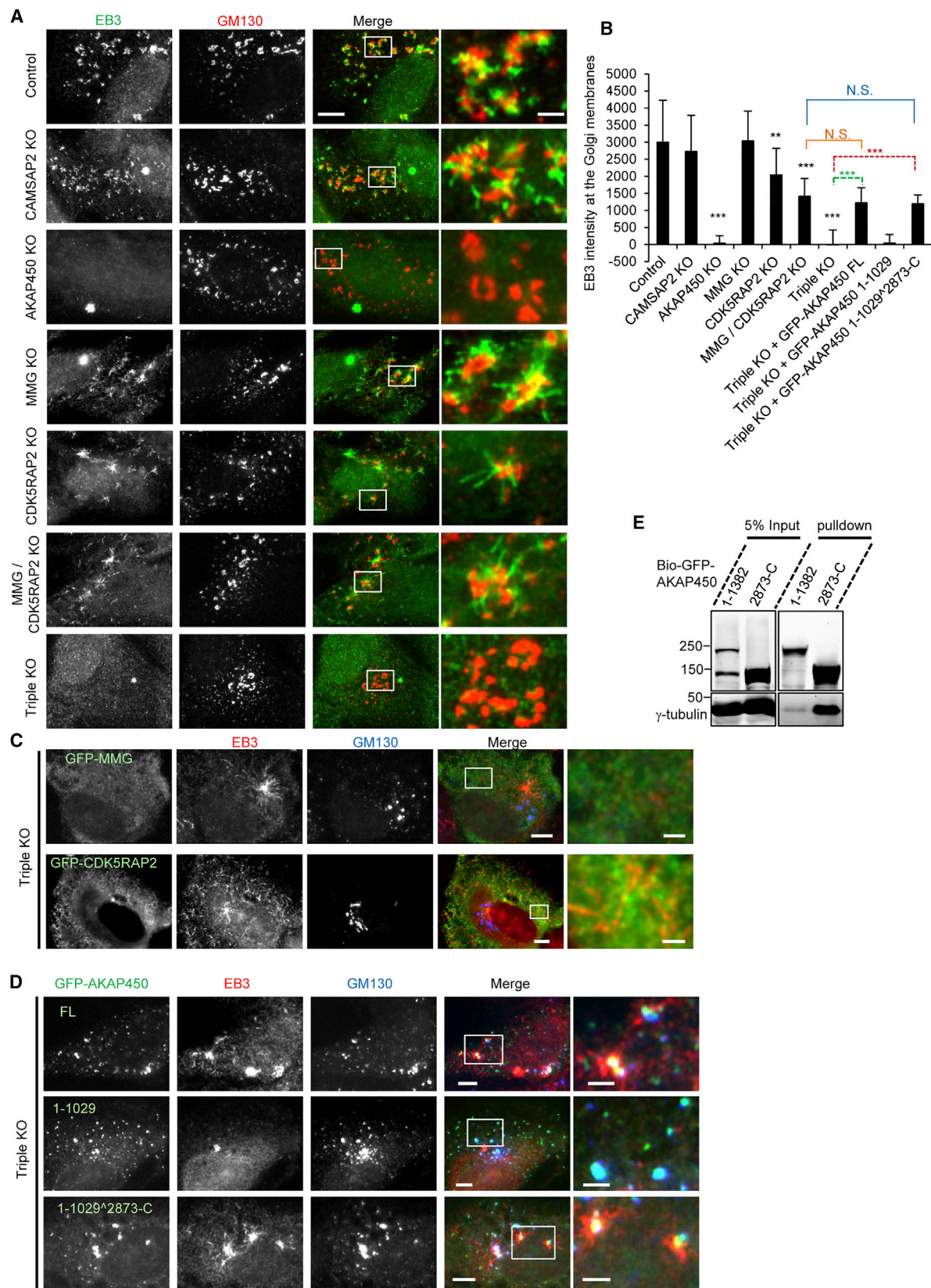
(C) Plots of average CAMSAP2 intensity in the Golgi area and outside the Golgi area in the indicated knockdown or KO cells expressed in a.u. Note that only the staining of CAMSAP2 at MT ends, and not the soluble pool of CAMSAP2, is quantified in this experiment, as in the methanol-fixed cells used here soluble CAMSAP2 cannot be detected. Thirty cells were analyzed per condition. Error bars represent SD. *** $p < 0.001$, Mann-Whitney U test.

(D) Quantification of CAMSAP2 and GM130 distribution in GCC185 KO or CLASP-depleted cells, analyzed and displayed as in Figure 1F.

(E) Immunostaining of α -tubulin (green) and GM130 (red) in the indicated knockdown or KO cells. Scale bar, 10 μ m.

(F) Quantification of α -tubulin and GM130 distribution in cells shown in (E), analyzed and displayed as in Figure 1F.

See also Figure S3.



(legend on next page)

the AKAP450 construct, in which the whole C-terminal quarter (amino acids 2,873–3,907) was fused to the N-terminal Golgi-targeting part (Figures 4B and 4D). Our mass spectrometry data showed that the C-terminal part of AKAP450 might interact with γ -TURC (Table S1), and we were able to confirm this observation by pull-down assays (Figure 4E). Fusions of shorter parts of AKAP450 C terminus (such as the minimal CAMSAP2-binding domain) to AKAP450 N terminus were insufficient for the rescue of MT nucleation and displayed no significant γ -TURC binding (not shown). This demonstrates distinct AKAP450 sequence requirements for different functions: the PACT domain (3,689–3,811) is sufficient for MMG binding, a larger C-terminal fragment (3,689–C) is needed for tethering CAMSAP2 stretches to the Golgi, and an even larger part (2,873–C) is required for MT nucleation. Furthermore, our data suggest that AKAP450 can recruit γ -TURC to the Golgi independently of CDK5RAP2 and MMG, although these two proteins improve nucleation efficiency and show some degree of redundancy.

Centriole Depletion Enhances γ -Tubulin Recruitment to the Golgi

Previous work has suggested that Golgi assembly relies on both centrosomal and Golgi-associated MTs (Vinogradova et al., 2012). To critically test the importance of both MT populations, we depleted centrioles in different KO lines using the Plk4 inhibitor centrinone, which blocks centriole duplication (Wong et al., 2015). In agreement with the published data (Wong et al., 2015), in these conditions RPE1 cells were arrested in G₁, and the large size of these cells allowed us to investigate Golgi morphology and MT association in detail. While centrioles were present in all control cells (data not shown), after 11 days of culture in the presence of centrinone, a large proportion (~90%) of control cells and all the single KO lines, with the exception of CDK5RAP2 KO, lost centrioles and centrosomes, judging by the staining for the centriole marker CEP135 and γ -tubulin (Figures 5A, S4A, and S4B). In contrast, the majority of cells lacking CDK5RAP2 that survived centrinone treatment still retained one centriole, which co-localized with γ -tubulin (Figures 5A and S4A). This suggests that the survival of acentrosomal cells depends on CDK5RAP2, possibly due to its roles in MT nucleation and spindle organization. Similarly, we could not efficiently deplete centrioles in any of the double- or triple-KO lines missing CDK5RAP2 (Figure 5A). Centriole depletion was also less efficient in the double AKAP450/CAMSAP2 KO (Figure 5A, and see below).

We next focused on the cell lines in which centrioles could be successfully depleted. In control cells, centrinone treatment

induced non-centrosomal MT organization and formation of extended Golgi ribbons consisting of distinct stacks, many of which strongly co-localized with CAMSAP2 stretches and spatially coincided with the region of high MT density (Figures 5B–5E). In centrinone-treated CAMSAP2 KO cells, MTs also lacked a single focus of convergence, while the Golgi acquired a reticulated appearance and displayed strong overlap with the regions of high MT density (Figures 5B, 5D, and 5E). Golgi-MT co-localization in CAMSAP2-depleted cells was much more prominent in centrinone-treated rather than untreated cells (Figures 3E, 5B, and 5E). Thus, in the absence of centrioles the Golgi takes over the MTOC function, and CAMSAP2 is no longer essential for the Golgi-MT association. We hypothesized that this was due to relocalization of some centrosomal proteins. Indeed, while we could not detect any enrichment of γ -tubulin at the Golgi in centrinone-untreated cells (not shown), clear γ -tubulin staining was observed on the Golgi membranes in centrinone-treated control and CAMSAP2 KO cells (Figures 5F, 5G, and S4C).

In Cells Lacking Centrosomes, AKAP450 and MMG Are Required for Co-organizing MTs and the Golgi but Not for the Coalescence of Golgi Membranes

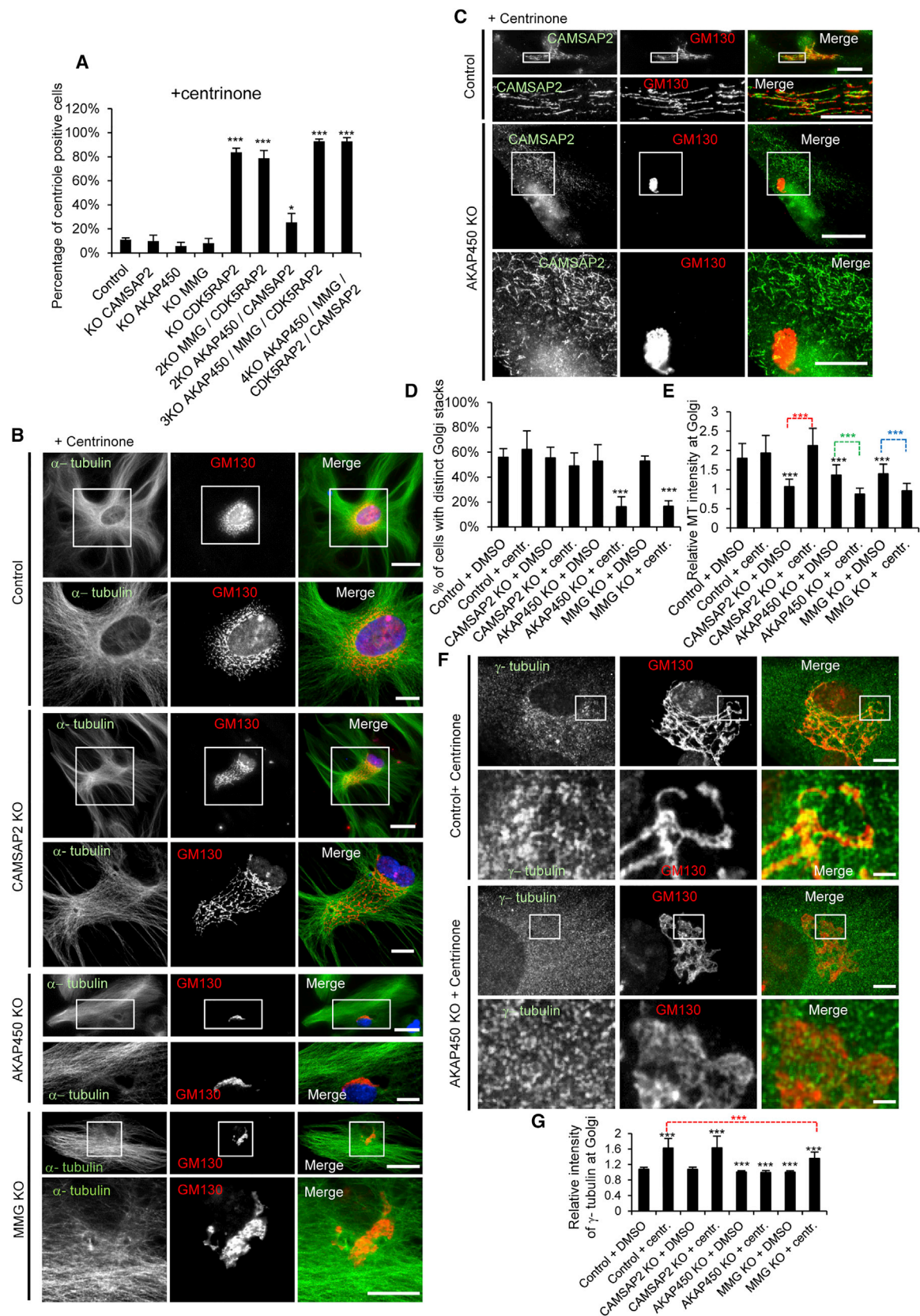
We next analyzed the effect of centrinone treatment on AKAP450 and MMG KO cell lines. In both cell lines, MTs formed a non-centrosomal network with MTs mostly aligned along the longest cell axis (Figure 5B). Strikingly, the MT density and CAMSAP2 stretches, which were located in the same cell areas (Figure S4D), were clearly separated from the Golgi apparatus (Figures 5B, 5C, 5E, and S4E). To our surprise, the Golgi was not dispersed in these conditions. On the contrary, it appeared as a highly compact structure typically located in the vicinity of the nucleus, and the individual Golgi stacks were difficult to distinguish (Figures 5B–5D and S4E). The enrichment of γ -tubulin at the Golgi membranes was weakened in MMG KO cells and abolished in AKAP450 KO cells (Figures 5F, 5G, and S4C).

Fully in line with these data, nocodazole washout experiments showed very strong MT nucleation from the Golgi fragments in control and CAMSAP2-depleted cells, while in AKAP450 KO cells MTs were nucleated from cytoplasmic sites distinct from the Golgi membranes (Figure S4F). Clearly visible, albeit somewhat reduced MT nucleation from the Golgi was observed in the single MMG or the double MMG/CDK5RAP2 KOs (Figure S4F), confirming that among the tested factors only AKAP450 is essential for Golgi-MT nucleation.

The large cell size slowed down Golgi reassembly after nocodazole washout in centrinone-treated cells. However, 2 hr after

Figure 4. Control of Golgi-MT Nucleation by AKAP450, MMG, and CDK5RAP2

- (A) Immunostaining of EB3 (green) and GM130 (red) in the indicated KO cells after 2.5 min of recovery from nocodazole-induced MT disassembly. Scale bars, 10 μ m (left) and 2 μ m (enlargements on the right).
- (B) Quantification of EB3 intensity at the GM130-positive membranes after 2.5 min of recovery from nocodazole-induced MT disassembly. Thirty Golgi-MT nucleation sites in 15–20 cells were analyzed per condition. Error bars represent SD. Values significantly different from each other are indicated by colored asterisks; black asterisks, comparison with control (***p < 0.001, **p < 0.01, Mann-Whitney U test) N.S., not significant.
- (C) Immunostaining of EB3 (red) and GM130 (blue) in AKAP450, MMG, and CDK5RAP2 triple-KO RPE1 cells transfected with GFP-MMG or GFP-CDK5RAP2 construct after 3 min of recovery from nocodazole-induced MT disassembly. Scale bars, 5 μ m and 1 μ m (enlargements on the right).
- (D) Immunostaining of EB3 (red) and GM130 (blue) after 2.5 min of recovery from nocodazole-induced MT disassembly in the AKAP450, MMG, and CDK5RAP2 triple-KO cells transfected with the indicated GFP-AKAP450 fusions. Bar, 5 μ m; zoomed-in images, bar, 2 μ m.
- (E) Streptavidin pull-down assays with the extracts of HEK293T cells co-expressing Bio-GFP-AKAP450 deletion mutants and BirA analyzed by western blotting with the antibodies to GFP and γ -tubulin.



(legend on next page)

nocodazole washout a single Golgi was recovered in all single KO cell lines, including the AKAP450 KO (Figures S5A and S5B; Movie S3). Small Golgi fragments became motile after nocodazole washout and gradually converged into larger ones, which became stretched out along MTs in control and CAMSAP2-depleted cells, but remained misshapen and clustered in AKAP450 KO cells.

To explore the details of Golgi organization in the absence of Golgi-anchored and centrosomal MTs, we analyzed Golgi structure by EM. At the EM level the Golgi apparatus is seen as a collection of stacks that together form the Golgi ribbon (Klumperman, 2011). Although Golgi morphology was different at the level of immunofluorescence staining (Figure 6A), no major differences in the shape and size of individual Golgi stacks could be detected by EM in different conditions (Figures 6B, 6C, and S6). However, we observed increased numbers of vesicles in the Golgi area in AKAP450 cells treated with centrinone, but not with DMSO (Figures 6B and S6), suggesting a possible vesicle trafficking defect. A similar trend was also observed in MMG KO cells (data not shown). These results demonstrate that a single Golgi apparatus can be assembled and maintained as a compact structure even when both the centrosomal and Golgi MTs are absent, but uncoupling of the Golgi from the MT mass might perturb vesicular trafficking.

Acentriolar MTOCs Organize MTs in Centrinone-Treated Cells Lacking Both AKAP450 and CAMSAP2

While centrinone treatment led to centriole loss in ~90% of cells lacking either AKAP450 or CAMSAP2, 25% of the double AKAP450/CAMSAP2 KO cells retained a CEP135-positive centriole (Figure 5A). Strikingly, 78% of these double-KO cells still contained a γ -tubulin cluster (Figure S4B). This γ -tubulin structure was strongly elongated, especially in acentriolar cells, co-localized with other centrosomal markers, such as pericentriolar and CDK5RAP2, and served as a major site for attachment of radially organized MTs (Figures 6D–6G). In the cells where no γ -tubulin cluster was present (22% of the population), MTs were strongly disorganized and their density was greatly reduced (Figures 6D–6G). The Golgi in the AKAP450/CAMSAP2 KO cells that had a γ -tubulin cluster was somewhat disorganized, similar to the AKAP450/CAMSAP2 KO cells that were not treated with centrinone, while in cells lacking a γ -tubulin cluster, Golgi consisted of scattered fragments (Figures 6E and 6H). We conclude that the centrosome, AKAP450-bound associated Golgi membranes and CAMSAP2 show redundancy in

organizing MT minus ends, and the presence of one of these factors is necessary and sufficient for the maintenance of a dense MT network, which, in turn, is required for organizing the Golgi.

Golgi-Anchored MTs Promote Cell Polarization and 3D Invasion

Previous work has shown that the loss of either CAMSAP2 or AKAP450 affected cell migration in monolayer wound-healing assays (Hurtado et al., 2011; Jiang et al., 2014; Rivero et al., 2009). Using our KO lines we confirmed these observations (Figure S7A). The first step of migration, cell polarization with the Golgi apparatus facing the wound, was less efficient in these cells than in control cells (Figures 7A and 7B). To address the underlying mechanism, we analyzed in detail the organization of the Golgi apparatus during cell reorientation. For CAMSAP2 KO cells, we focused only on the cells where the Golgi was localized predominantly on one side of the nucleus, allowing unambiguous quantification of Golgi orientation. We found that in control cells Golgi reorientation was typically accompanied by the separation of the Golgi into smaller stacks that moved independently along and sometimes across the nucleus (Figures 7A and 7C; Movie S4). In contrast, in CAMSAP2- and AKAP450-depleted cells, reorientation occurred while the Golgi largely maintained its organization and gradually turned around the nucleus, with CAMSAP2 stretches accumulating around but not at the Golgi (Figures 7A, 7C, and S7B; Movies S5 and S6).

To test the importance of Golgi-MT-based cell polarization in a more physiological context, we next turned to cancer cell invasion in a 3D collagen matrix. For these experiments we used highly invasive HT1080 fibrosarcoma cells, which displayed prominent AKAP450- and MMG-dependent localization of CAMSAP2 stretches to the Golgi, very similar to RPE1 cells (Figures S7C and S7D). Strikingly, the velocity of cell movement in a 3D collagen matrix was reduced more than 3-fold in CAMSAP2-depleted cells and 5-fold in AKAP450-depleted cells, with a milder but comparable phenotype observed after MMG depletion (Figures 7D and 7E). This effect strongly correlated with the loss of polarized cell shape: while motile control cells typically extended one elongated invasive pseudopod, multiple shorter pseudopods were observed in cells lacking CAMSAP2, AKAP450, and MMG (Figure 7F). We conclude that the attachment of non-centrosomal MTs to the Golgi is required for the effective cell polarization, which becomes particularly important when cells invade a 3D matrix.

Figure 5. Effects of Centrosome Depletion on MT-Golgi Co-organization

(A) Percentage of centriole-positive cells, based on CEP135 staining, in the indicated cell lines after 11 days treatment with 125 nM centrinone. A total of 57–188 cells were analyzed per condition. Error bars represent SD. * $p < 0.05$, *** $p < 0.001$, Student's *t* test.

(B and C) Immunostaining of α -tubulin (B) (green), CAMSAP2 (C) (green), and GM130 (red) in the indicated centrinone-treated cell lines. Scale bars, 50 μ m (upper panels) and 20 μ m (enlargements).

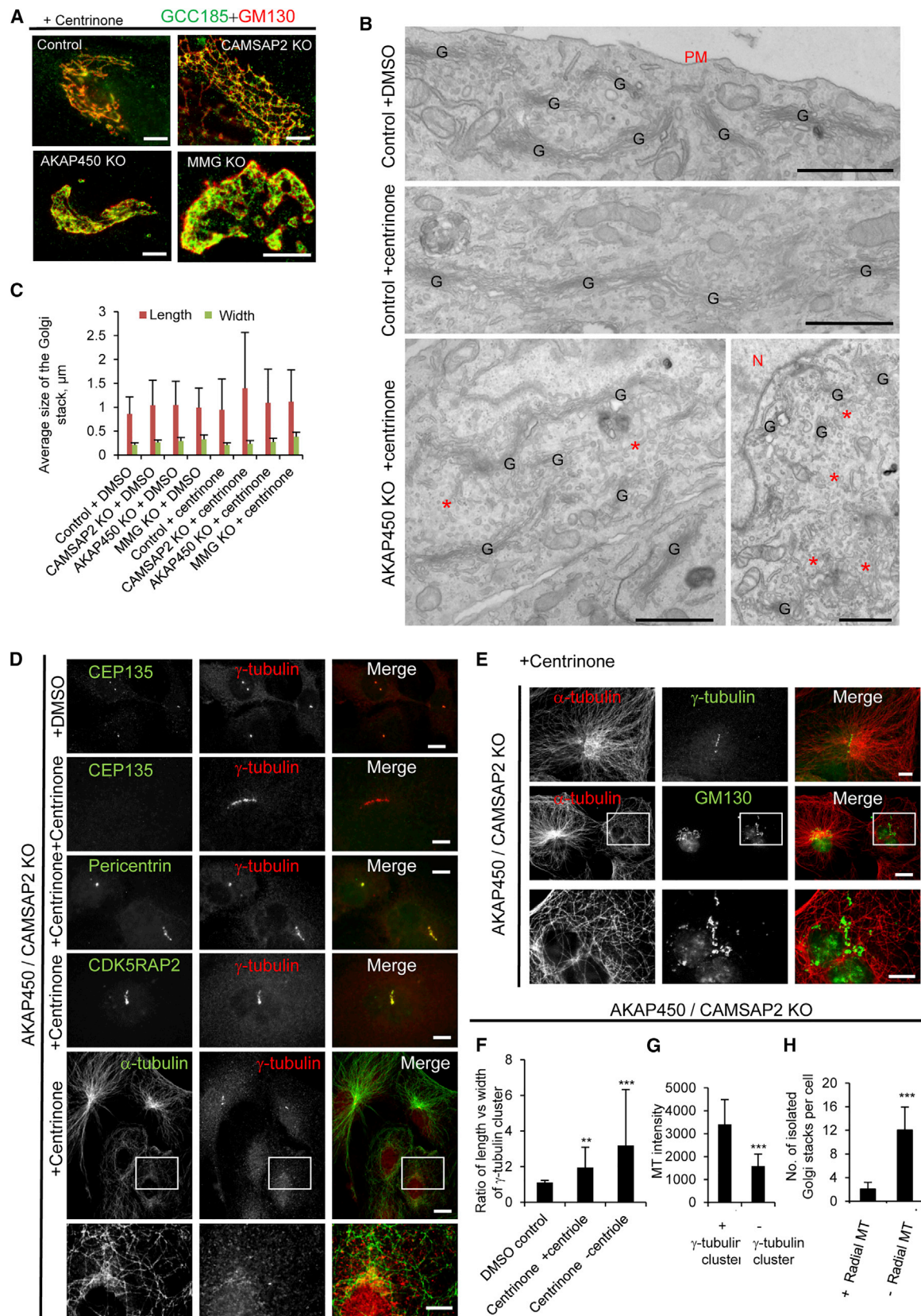
(D) Percentage of cells with distinct small Golgi stacks in the indicated cells and conditions. A total of 110–360 cells were analyzed per condition. Error bars represent SD. *** $p < 0.001$, Mann-Whitney U test.

(E) Ratios of the average MT intensities in the Golgi area and in the cytoplasm in the indicated cells and conditions. Thirty cells were analyzed per condition. Error bars represent SD. *** $p < 0.001$, Mann-Whitney U test.

(F) Immunostaining of γ -tubulin (green) and GM130 (red) in the indicated centrinone-treated cell lines. Scale bars, 10 μ m and in the enlargements, 2 μ m.

(G) Ratio of the average intensity of γ -tubulin staining at the Golgi and in the cytoplasm. In the absence of enrichment of γ -tubulin staining at the Golgi, this ratio is close to 1. Thirty cells were analyzed per condition. Plots are presented as in (D).

See also Figures S4 and S5; Movie S3.



(legend on next page)

DISCUSSION

In this study, we have identified an essential role of the MT minus-end stabilizing protein CAMSAP2 in organizing MTs at the Golgi. Combined with a series of KO and rescue experiments, this finding allowed us to generate a model of how Golgi MTs are formed and maintained (Figures 7G and 7H). In accordance with previously published data, the key factor in Golgi-MT organization is AKAP450 located at the *cis* Golgi (Hurtado et al., 2011; Rivero et al., 2009). AKAP450 regulates Golgi MTs through several mechanisms: by promoting MT nucleation at the Golgi membranes, likely through binding to γ -TURC, by recruiting MT nucleation-promoting factors MMG and CDK5RAP2, and by acting in a complex with MMG to enable the association of CAMSAP2-positive MT minus ends with the Golgi membranes. The latter function is crucial, because despite the fact that MTs can be efficiently nucleated at the Golgi in the absence of CAMSAP2, the minus ends of these MTs are not stable enough and are not retained at the Golgi, so that only centrosomal MTs persist if CAMSAP2 is absent.

It is likely that additional proteins contribute to the interaction between the Golgi and MTs. Since CAMSAP2-decorated MT lattices can be quite long (~ 1 – $3\ \mu\text{m}$) and can span different Golgi compartments, these additional factors can localize to different parts of the Golgi, such as CLASPs, which are targeted to the *trans*-Golgi by GCC185 (Efimov et al., 2007), and MTCL1, which can interact with both AKAP450 and CLASPs (Sato et al., 2014). The major impact of CLASPs, however, appears to be not through MT tethering but through stabilization of CAMSAP2 stretches, which become less numerous or even disappear in CLASP knockdown cells. The removal of CLASPs from the Golgi by GCC185 KO had no effect on the organization of CAMSAP2 stretches at the Golgi, indicating that cytoplasmic CLASP is sufficient to stabilize CAMSAP2-bound MTs at the Golgi. It is possible that CLASPs promote MT outgrowth from pre-existing templates, as was recently shown for XMAP215 (Wieczorek et al., 2015), which, similar to CLASPs, has tubulin-binding TOG domains. CLASPs might enhance the stability of CAMSAP2-decorated MT lattices by facilitating efficient MT polymerization from their ends. The generation of KO lines has allowed us to test the relative importance of different factors in MT nucleation and MT minus-end stabilization. We found that centrioles could not be depleted in CDK5RAP2 KO cells, indicating that CDK5RAP2 is required for cell division or survival in the absence of centrosomes, in agreement with its important

role in MT nucleation (Choi et al., 2010). We also explored the competition and redundancy between the centrosome, the Golgi, and CAMSAP2-dependent stabilization in organizing MT minus ends. We found that one or even two of these factors can be removed without a major impact on cell viability, because the other pathways become more dominant.

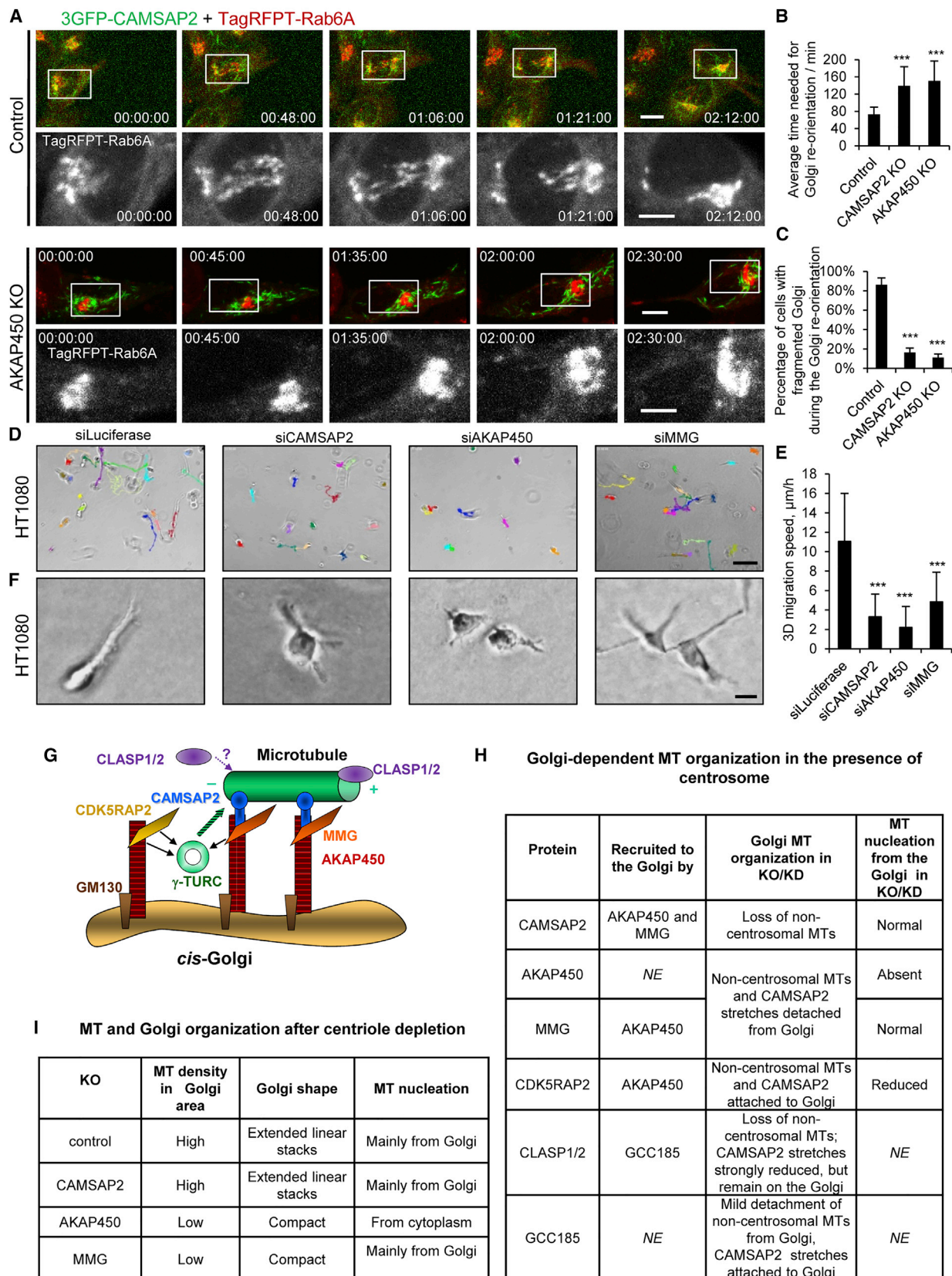
It is important to note that our centriole depletion experiments are fundamentally different from the previously conducted centrosome ablation assays (Efimov et al., 2007; Vinogradova et al., 2012), because Plk4 inhibition leads to the loss of centrioles but not the centrosome-associated proteins, which can relocate to other cellular sites. For example, when centrosome function is removed the MT-organizing capacity of the Golgi increases, possibly due to the enhanced AKAP450-dependent recruitment of γ -tubulin. This observation has important implications for understanding MT organization in differentiated cell types, such as, for example, neurons, in which the centrosomes become inactivated during differentiation (Kapitein and Hoogenraad, 2015).

In acenrosomal cells, the link between CAMSAP2 and the Golgi becomes less critical, as the Golgi still co-localizes with the MT mass in CAMSAP2 KO cells after centrione treatment. In this situation, an additional connection between Golgi membranes and MTs might be provided by the EB1, which binds to MMG (Roubin et al., 2013; Wang et al., 2014). The importance of such a connection in acenrosomal cells would explain why in MMG KO cells treated with centrione, Golgi is disconnected from the MT mass despite the fact that Golgi membranes can still recruit some γ -tubulin and nucleate MTs after nocodazole washout (Figure 7I).

When both centrosomes and Golgi-derived AKAP450- or MMG-dependent MTs are absent, MTs still form dense and reasonably organized arrays, with their minus ends stabilized by CAMSAP2. Similar redundancy between MT minus-end stabilization pathways dependent on γ -tubulin and the CAMSAP2 homolog Patronin has been also observed in worms (Wang et al., 2015). Furthermore, when both CAMSAP2 and the AKAP450-dependent Golgi-MT interactions were abolished and centrioles depleted, the cells could only maintain dense MT networks by expanding the acenrosomal centrosome into an abnormally shaped linear structure. It is likely that such expansion of the pericentrosomal material allows more MT minus ends to be attached and stabilized, and thus MT density can be maintained in the absence of non-centrosomal minus-end stabilization pathways. Together, these data illustrate the

Figure 6. Effects of Centriole Depletion in AKAP450 and CAMSAP2 KO Cells

- (A) Immunostaining of GCC185 (green) and GM130 (red) in the indicated centrione-treated cell lines. Scale bar, 10 μm .
 (B) EM images of Golgi stacks in cells treated as indicated. G, individual Golgi stacks; N, nucleus; *, vesicular areas; PM, plasma membrane. Scale bars, 1 μm .
 (C) Quantification of Golgi stack length and width, measured from EM images. Error bars represent SD of 27–38 Golgi stacks in ten cell profiles analyzed per condition.
 (D) Immunostaining of CEP135 (green), pericentrin (green), CDK5RAP2 (green), α -tubulin (green), and γ -tubulin (red) in AKAP450/CAMSAP2 double-KO RPE1 cells that were treated with DMSO or centrione. Scale bar, 10 μm and in the enlargements, 5 μm .
 (E) Immunostaining of α -tubulin (red), γ -tubulin (green), and GM130 (green) in AKAP450/CAMSAP2 double-KO RPE1 cells that were treated with centrione. Scale bar, 10 μm and in the enlargements, 5 μm .
 (F) Ratio of γ -tubulin cluster length and width in AKAP450/CAMSAP2 double-KO RPE1 cells that were treated with DMSO or centrione.
 (G) Average MT intensity in γ -tubulin cluster positive and negative AKAP450/CAMSAP2 double-KO RPE1 cells that were treated with centrione.
 (H) Average number of isolated Golgi stacks per cell in AKAP450/CAMSAP2 double-KO RPE1 cells with radial or non-radial MTs.
 In (F)–(H), error bars represent SD and 22–40 cells were analyzed per condition. **p < 0.01, ***p < 0.001, Mann-Whitney U test.
 See also Figure S6.



(legend on next page)

flexibility and partial redundancy of MT minus-end organization mechanisms and also show that at least one of these mechanisms needs to be present to maintain dense MT arrays.

Use of KO lines also allowed us to test the importance of centrosomal, non-centrosomal, and Golgi-anchored MT populations for Golgi maintenance. We found that the Golgi was more compact in the single AKAP450 KO than in the single CAMSAP2 and double AKAP450/CAMSAP2 KO, suggesting that non-centrosomal CAMSAP2-stabilized MTs might contribute to organizing Golgi membranes even when they are not anchored to them. It is possible that the presence of abundant non-centrosomal MTs promotes lateral movements of Golgi stacks and facilitates their interactions, compared with predominantly centripetal movements, which occur when all MTs are attached to the centrosome. In agreement with this idea, we found that Golgi membranes could be assembled into a single structure and became even more compact when both centrosomal and Golgi-anchored MTs were removed, but abundant non-centrosomal MTs were still present, which was the case in centrinone-treated AKAP450 and MMG KO cells (Figure 7I). Live imaging experiments showed that dispersed Golgi fragments could effectively coalesce in these conditions but were not stretched into linear patterns, in contrast to control or CAMSAP2 KO cells. These data suggest that Golgi MTs participate not only in bringing the individual Golgi stacks together (Rios, 2014; Sanders and Kaverina, 2015; Zhu and Kaverina, 2013) but also in shaping Golgi ribbons. At the EM level, the size of individual Golgi stacks remained unchanged, but more vesicles were present in the Golgi area, suggesting that vesicle trafficking might be affected by the low MT density and MT disorganization in the Golgi vicinity due to simultaneous absence of centrosomal and Golgi-anchored MTs. Finally, we found that the Golgi organization could not be supported by the very sparse and disorganized MT network in cells simultaneously lacking the centrosome-, CAMSAP2-, and AKAP450-dependent Golgi-tethered MTs. We note that since these cells represented the minor part (22%) of the total cell population, it is possible that their viability was compromised.

The importance of Golgi-anchored MTs is further illustrated by the analysis of switching of cell polarity. Surprisingly, the presence of Golgi-anchored MTs facilitated rather than prevented temporary splitting of the Golgi, which could then be efficiently repositioned to the front side of the nucleus. It is possible that the presence of Golgi-connected non-centrosomal

MTs facilitates motility of the Golgi membranes by creating MT-based pulling forces and enhancing the structural flexibility of the Golgi apparatus. The polarity defects observed upon the loss of Golgi-anchored MTs had only a modest effect on cell motility in 2D but exerted a much more profound impact on the ability of cells to undergo invasive movement in a 3D matrix, indicating that further studies of the impact of Golgi MTs should focus on 3D cell models. We note that in this study we focused on cells undergoing mesenchymal motility and that other motility types, such as amoeboid motility, which are less dependent on MT networks, might not require Golgi MTs. In line with this idea, recent work showed that AKAP450 is not needed for T cell migration into tissues and lymph nodes, although its loss did affect T cell receptor recycling (Herter et al., 2015). Furthermore, a mouse KO study showed that while AKAP450 is essential for spermatogenesis and Sertoli cell maturation, it is not required for mouse viability (Schimenti et al., 2013). This is in agreement with our finding that AKAP450 KO cells are viable and display no major cell-cycle defects, and suggests that the cell-intrinsic polarity defects that we observed in cultured AKAP450 KO cells might be compensated during tissue development, possibly due to extrinsic cell polarization cues.

To conclude, we have shown how a complex interplay between MT end-binding proteins and associated factors allows the Golgi to act as a dynamic MTOC. The tools described in our study will likely contribute to revealing the full complexity of organelle-driven MT organization.

EXPERIMENTAL PROCEDURES

The description of the details of cell culture and transfection, DNA constructs, drug treatments, antibodies, EM, and mass spectrometry analysis can be found in [Supplemental Experimental Procedures](#).

Generation of RPE1 KO Cell Lines

RPE1 KO cell lines were generated by transfecting the cells with the pSpCas9(BB)-2A-Puro (PX459) (Ran et al., 2013) vector bearing the appropriate targeting sequences using Fugene 6. One day after transfection, cells were subjected to selection with 25 μ g/mL puromycin for 3 days. After selection, cells were allowed to recover in normal medium for \sim 7 days, and the efficiency of KO was checked by immunofluorescence staining. Depending on the efficiency, 24–100 individual clones were isolated and characterized by western blotting and immunofluorescence staining. RPE1 MMG and CDK5RAP2 double-KO cell line was generated based on CDK5RAP2 KO; AKAP450, MMG, and CDK5RAP2 triple-KO and AKAP450, MMG, CDK5RAP2,

Figure 7. CAMSAP2 and AKAP450 Promote Efficient Cell Polarization and Migration

(A) Live images of control or AKAP450 KO cells co-expressing 3 \times GFP-CAMSAP2 and TagRFP-T-Rab6A during cell reorientation. Scale bars, 10 μ m (upper panels) and 5 μ m (enlargements).

(B and C) Monolayer wound-healing assay. Time needed for Golgi reorientation (42–48 cells analyzed per condition) (B) and the percentage of cells with fragmented Golgi during Golgi reorientation (C) in control or the indicated KO cells (118–135 cells analyzed per condition in three to five experiments). Error bars represent SD. *** p < 0.001, Mann-Whitney U test (B) or Student's t test (C).

(D) Tracking of control, CAMSAP2, AKAP450, or MMG-knockdown HT1080 cells grown in a 3D collagen matrix and imaged by phase contrast. Scale bar, 100 μ m.

(E) Average migration velocity of control/CAMSAP2-knockdown/AKAP450-knockdown/MMG-knockdown HT1080 in 3D-matrix culture. Error bars represent SD of 20–24 cells analyzed per condition. *** p < 0.001, Mann-Whitney U test.

(F) Morphology of control/CAMSAP2-knockdown/AKAP450-knockdown/MMG-knockdown HT1080 in 3D-matrix culture. Scale bar, 10 μ m.

(G) Model of the molecular mechanism of MT organization at the *cis* Golgi. AKAP450, which is targeted to the Golgi by GM130, controls MT nucleation by recruiting γ -TURC directly or through CDK5RAP2 and MMG. CAMSAP2 stabilizes free MT minus ends and attaches them to Golgi membranes through a complex of AKAP450 and MMG. CLASPs promote stability of CAMSAP2-bound MT stretches by acting at the MT plus end and possibly also the minus end. The interaction of CLASPs with the *trans*-Golgi-bound GCC185 likely makes this process more efficient and can contribute to MT tethering (not depicted).

(H and I) Summarizing tables of MT and Golgi phenotypes observed in different KO lines. NE, not examined in this study.

See also [Figure S7](#) and [Movies S4](#), [S5](#), and [S6](#).

and CAMSAP2KO quadruple-KO cell lines were subsequently made by knocking out first AKAP450 and then CAMSAP2 in this double-KO line; AKAP450 and CAMSAP2 double-KO cell line was generated based on AKAP450 KO.

Image Acquisition

Images of fixed cells were collected with a Nikon Eclipse 80i equipped with a Plan Apo VC 100 × 1.4 numerical aperture (NA), 60 × 1.4 NA, or Plan Fluor 40 × 1.3 NA. oil objectives and a CoolSNAP HQ2 camera (Roper Scientific), driven by Nikon NIS (Br) elements software.

3D-SIM images of fixed samples were acquired on a commercial structured illumination microscope (DeltaVision OMX v4.0 BLAZE, GE Healthcare) equipped with pco.edge sCMOS cameras (PCO) and 60× NA 1.49 Olympus objective. Thirty to forty z slices with a distance of 125 nm were acquired using 488- and 568-nm lasers and corresponding FITC/mCherry excitation and emission combinations of OMX filters. Color-channel registration and image reconstruction were performed using the SoftWoRx v6.2 package from GE Healthcare.

Live-cell images were collected with spinning-disk microscopy, which was performed on an inverted research microscope Nikon Eclipse Ti-E (Nikon) with the perfect focus system (PFS) (Nikon), equipped with Plan Apo VC 100× NA 1.40 oil objective (Nikon), CSU-X1-A1 Spinning Disc (Yokogawa), and Photometrics Evolve 512 EMCCD camera (Roper Scientific), controlled by MetaMorph 7.7 software (Molecular Devices). Images were projected onto the camera chip with intermediate lens 2.0× (Edmund Optics) at a magnification of 0.067 $\mu\text{m}/\text{pixel}$. To keep cells at 37°C we used the stage top incubator INUBG2E-ZILCS (Tokai Hit). The microscope was equipped with a custom-ordered illuminator (Nikon, MEY10021) modified by Roper Scientific France/PICT-IBISA, Institut Curie. A 491-nm (100 mW) Calypso (Cobolt) and a 561-nm (100 mW) Jive (Cobolt) laser were used for excitation. The spinning disk was equipped with a 405–491–561 triple-band mirror and GFP, mCherry, and GFP/mCherry emission filters (Chroma). For simultaneous imaging of green and red fluorescence we used an ET-mCherry/GFP filter set (59022, Chroma) together with the DualView (DV2, Roper) equipped with the dichroic filter 565dcxr (Chroma) and HQ530/30m emission filter (Chroma).

Phase-contrast and wide-field fluorescence live-cell imaging were performed on a Nikon Ti equipped with the PFS (Nikon), a super high-pressure mercury lamp (C-SHG1, Nikon), Lambda SC Smart Shutter controllers (Sutter), a Plan Apochromat DM 20× NA 0.75 (Ph2) or a Plan Fluor DLL 10× NA 0.3 (Ph1), an ET-mCherry filter (Chroma), a CoolSNAP HQ2 7 CCD camera (Photometrics), a motorized stage MS-2000-XYZ with Piezo Top Plate (ASI) and a stage top incubator INUG2E-ZILCSD-DV (Tokai Hit) for 37°C/5% CO₂ incubation. The microscope setup was controlled by the open-source microscopy software Micro-Manager.

Image Preparation and Analysis

Images were prepared by using MetaMorph, ImageJ, and Adobe Photoshop. All images were modified by adjustments of levels and contrast. ImageJ was used for quantification of the immunofluorescence signal intensity. Statistical comparisons were performed in SigmaPlot using the Rank-Sum Test function (Mann-Whitney U test).

The ImageJ Radial Profile plugin was used to measure the distribution of immunofluorescence signal intensity along the radius. A circle with a radius of 14.79 μm was drawn with the center positioned at the center of the Golgi, and the intensity profile along the radius was obtained. For each cell, the position of the circle was the same for different channels (GM130, CAMSAP2, and α -tubulin). The fluorescence intensity values for each profile were normalized (the highest value was taken for 100%, the lowest value for 0). EM images were analyzed in ImageJ.

SUPPLEMENTAL INFORMATION

Supplemental Information includes Supplemental Experimental Procedures, seven figures, one table, and six movies and can be found with this article online at <http://dx.doi.org/10.1016/j.devcel.2016.08.009>.

AUTHOR CONTRIBUTIONS

J.W. designed and conducted the experiments and wrote the paper; C.d.H. and J.K. performed and analyzed EM experiments; B.P.B., I.N., K.J., S.H.,

M.M., and C.Y. contributed tools and conducted the experiments; I.G. and E.A.K. contributed to imaging experiments; Q.L. and A.F.M.A. performed mass spectrometry experiments and their analysis; C.C.H. and R.Z.Q. contributed tools and wrote the paper; A.A. designed and supervised the study and wrote the paper.

ACKNOWLEDGMENTS

We thank A. Shiao and T. Gahman (Small Molecule Discovery Program, Ludwig Institute for Cancer Research, San Diego, CA, USA), M. Takahashi (TEIKYO, Tokyo, Japan), E. Bindels (Erasmus MC, Rotterdam, the Netherlands), and R. Weinberg (Whitehead Institute, USA) for the gift of materials, J. Demmers (Erasmus MC, Rotterdam, the Netherlands) for help with mass spectrometry, and R. Szwaneke (Cell Biology UMC Utrecht) for preparation of the EM images. This study was supported by China Scholarship Council scholarships to J.W. and C.Y.; the Netherlands Organization for Scientific Research (NWO) through a VIDI grant (723.012.102) and as part of the Netherlands (project number 184.032.201) to A.F.M.A.; and NWO-CW ECHO grant (711.011.005) to A.A.

Received: February 20, 2016

Revised: May 23, 2016

Accepted: August 21, 2016

Published: September 22, 2016

REFERENCES

- Akhmanova, A., and Hoogenraad, C.C. (2015). Microtubule minus-end-targeting proteins. *Curr. Biol.* 25, R162–R171.
- Chabin-Brion, K., Marceiller, J., Perez, F., Settegrana, C., Drechou, A., Durand, G., and Pous, C. (2001). The Golgi complex is a microtubule-organizing organelle. *Mol. Biol. Cell* 12, 2047–2060.
- Choi, Y.K., Liu, P., Sze, S.K., Dai, C., and Qi, R.Z. (2010). CDK5RAP2 stimulates microtubule nucleation by the gamma-tubulin ring complex. *J. Cell Biol.* 191, 1089–1095.
- Conduit, P.T., Wainman, A., and Raff, J.W. (2015). Centrosome function and assembly in animal cells. *Nat. Rev. Mol. Cell Biol.* 16, 611–624.
- Efimov, A., Kharitonov, A., Efimova, N., Loncarek, J., Miller, P.M., Andreyeva, N., Gleeson, P., Galjart, N., Maia, A.R., McLeod, I.X., et al. (2007). Asymmetric CLASP-dependent nucleation of noncentrosomal microtubules at the trans-Golgi network. *Dev. Cell* 12, 917–930.
- Gillingham, A.K., and Munro, S. (2000). The PACT domain, a conserved centrosomal targeting motif in the coiled-coil proteins AKAP450 and pericentrin. *EMBO Rep.* 1, 524–529.
- Herter, J.M., Grabie, N., Cullere, X., Azcutia, V., Rosetti, F., Bennett, P., Herter-Sprie, G.S., Elyaman, W., Lusinskas, F.W., Lichtman, A.H., et al. (2015). AKAP9 regulates activation-induced retention of T lymphocytes at sites of inflammation. *Nat. Commun.* 6, 10182.
- Hurtado, L., Caballero, C., Gavilan, M.P., Cardenas, J., Bornens, M., and Rios, R.M. (2011). Disconnecting the Golgi ribbon from the centrosome prevents directional cell migration and ciliogenesis. *J. Cell Biol.* 193, 917–933.
- Jiang, K., Hua, S., Mohan, R., Grigoriev, I., Yau, K.W., Liu, Q., Katrukha, E.A., Altaalar, A.F., Heck, A.J., Hoogenraad, C.C., et al. (2014). Microtubule minus-end stabilization by polymerization-driven CAMSAP deposition. *Dev. Cell* 28, 295–309.
- Kapitein, L.C., and Hoogenraad, C.C. (2015). Building the neuronal microtubule cytoskeleton. *Neuron* 87, 492–506.
- Klumperman, J. (2011). Architecture of the mammalian Golgi. *Cold Spring Harb. Perspect. Biol.* 3, <http://dx.doi.org/10.1101/cshperspect.a005181>.
- Miller, P.M., Folkmann, A.W., Maia, A.R., Efimova, N., Efimov, A., and Kaverina, I. (2009). Golgi-derived CLASP-dependent microtubules control Golgi organization and polarized trafficking in motile cells. *Nat. Cell Biol.* 11, 1069–1080.
- Mimori-Kiyosue, Y., Grigoriev, I., Lansbergen, G., Sasaki, H., Matsui, C., Severin, F., Galjart, N., Grosveld, F., Vorobjev, I., Tsukita, S., et al. (2005).

- CLASP1 and CLASP2 bind to EB1 and regulate microtubule plus-end dynamics at the cell cortex. *J. Cell Biol.* 168, 141–153.
- Nagae, S., Meng, W., and Takeichi, M. (2013). Non-centrosomal microtubules regulate F-actin organization through the suppression of GEF-H1 activity. *Genes Cells* 18, 387–396.
- Nakamura, N., Wei, J.H., and Seemann, J. (2012). Modular organization of the mammalian Golgi apparatus. *Curr. Opin. Cell Biol.* 24, 467–474.
- Oddoux, S., Zaal, K.J., Tate, V., Kenea, A., Nandkeolyar, S.A., Reid, E., Liu, W., and Ralston, E. (2013). Microtubules that form the stationary lattice of muscle fibers are dynamic and nucleated at Golgi elements. *J. Cell Biol.* 203, 205–213.
- Ori-McKenney, K.M., Jan, L.Y., and Jan, Y.N. (2012). Golgi outposts shape dendrite morphology by functioning as sites of acentrosomal microtubule nucleation in neurons. *Neuron* 76, 921–930.
- Overholtzer, M., Zhang, J., Smolen, G.A., Muir, B., Li, W., Sgroi, D.C., Deng, C.X., Brugge, J.S., and Haber, D.A. (2006). Transforming properties of YAP, a candidate oncogene on the chromosome 11q22 amplicon. *Proc. Natl. Acad. Sci. USA* 103, 12405–12410.
- Ran, F.A., Hsu, P.D., Wright, J., Agarwala, V., Scott, D.A., and Zhang, F. (2013). Genome engineering using the CRISPR-Cas9 system. *Nat. Protoc.* 8, 2281–2308.
- Rios, R.M. (2014). The centrosome-Golgi apparatus nexus. *Philos. Trans. R. Soc. Lond. B Biol. Sci.* 369.
- Rivero, S., Cardenas, J., Bornens, M., and Rios, R.M. (2009). Microtubule nucleation at the cis-side of the Golgi apparatus requires AKAP450 and GM130. *EMBO J.* 28, 1016–1028.
- Roubin, R., Acquaviva, C., Chevrier, V., Sedjai, F., Zyss, D., Birnbaum, D., and Rosnet, O. (2013). Myomegalin is necessary for the formation of centrosomal and Golgi-derived microtubules. *Biol. Open* 2, 238–250.
- Sanders, A.A., and Kaverina, I. (2015). Nucleation and dynamics of golgi-derived microtubules. *Front Neurosci.* 9, 431.
- Sato, Y., Hayashi, K., Amano, Y., Takahashi, M., Yonemura, S., Hayashi, I., Hirose, H., Ohno, S., and Suzuki, A. (2014). MTCL1 crosslinks and stabilizes non-centrosomal microtubules on the Golgi membrane. *Nat. Commun.* 5, 5266.
- Schimenti, K.J., Feuer, S.K., Griffin, L.B., Graham, N.R., Bovet, C.A., Hartford, S., Pendola, J., Lessard, C., Schimenti, J.C., and Ward, J.O. (2013). AKAP9 is essential for spermatogenesis and Sertoli cell maturation in mice. *Genetics* 194, 447–457.
- Schmidt, P.H., Dransfield, D.T., Claudio, J.O., Hawley, R.G., Trotter, K.W., Milgram, S.L., and Goldenring, J.R. (1999). AKAP350, a multiply spliced protein kinase A-anchoring protein associated with centrosomes. *J. Biol. Chem.* 274, 3055–3066.
- Takahashi, M., Shibata, H., Shimakawa, M., Miyamoto, M., Mukai, H., and Ono, Y. (1999). Characterization of a novel giant scaffolding protein, CG-NAP, that anchors multiple signaling enzymes to centrosome and the Golgi apparatus. *J. Biol. Chem.* 274, 17267–17274.
- Takahashi, M., Yamagiwa, A., Nishimura, T., Mukai, H., and Ono, Y. (2002). Centrosomal proteins CG-NAP and kendrin provide microtubule nucleation sites by anchoring gamma-tubulin ring complex. *Mol. Biol. Cell* 13, 3235–3245.
- Tanaka, N., Meng, W., Nagae, S., and Takeichi, M. (2012). Nezha/CAMSAP3 and CAMSAP2 cooperate in epithelial-specific organization of noncentrosomal microtubules. *Proc. Natl. Acad. Sci. USA* 109, 20029–20034.
- Toya, M., Kobayashi, S., Kawasaki, M., Shioi, G., Kaneko, M., Ishiuchi, T., Misaki, K., Meng, W., and Takeichi, M. (2016). CAMSAP3 orients the apical-to-basal polarity of microtubule arrays in epithelial cells. *Proc. Natl. Acad. Sci. USA* 113, 332–337.
- Vinogradova, T., Miller, P.M., and Kaverina, I. (2009). Microtubule network asymmetry in motile cells: role of Golgi-derived array. *Cell Cycle* 8, 2168–2174.
- Vinogradova, T., Paul, R., Grimaldi, A.D., Loncarek, J., Miller, P.M., Yampolsky, D., Magidson, V., Khodjakov, A., Mogilner, A., and Kaverina, I. (2012). Concerted effort of centrosomal and Golgi-derived microtubules is required for proper Golgi complex assembly but not for maintenance. *Mol. Biol. Cell* 23, 820–833.
- Wang, Z., Wu, T., Shi, L., Zhang, L., Zheng, W., Qu, J.Y., Niu, R., and Qi, R.Z. (2010). Conserved motif of CDK5RAP2 mediates its localization to centrosomes and the Golgi complex. *J. Biol. Chem.* 285, 22658–22665.
- Wang, Z., Zhang, C., and Qi, R.Z. (2014). A newly identified myomegalin isoform functions in Golgi microtubule organization and ER-Golgi transport. *J. Cell Sci.* 127, 4904–4917.
- Wang, S., Wu, D., Quintin, S., Green, R.A., Cheerambathur, D.K., Ochoa, S.D., Desai, A., and Oegema, K. (2015). NOCA-1 functions with gamma-tubulin and in parallel to Patronin to assemble non-centrosomal microtubule arrays in *C. elegans*. *Elife* 4, e08649.
- Wieczorek, M., Bechstedt, S., Chaaban, S., and Brouhard, G.J. (2015). Microtubule-associated proteins control the kinetics of microtubule nucleation. *Nat. Cell Biol.* 17, 907–916.
- Witczak, O., Skälhegg, B.S., Keryer, G., Bornens, M., Tasken, K., Jahnsen, T., and Orstavik, S. (1999). Cloning and characterization of a cDNA encoding an A-kinase anchoring protein located in the centrosome, AKAP450. *EMBO J.* 18, 1858–1868.
- Wong, Y.L., Anzola, J.V., Davis, R.L., Yoon, M., Motamedi, A., Kroll, A., Seo, C.P., Hsia, J.E., Kim, S.K., Mitchell, J.W., et al. (2015). Cell biology. Reversible centriole depletion with an inhibitor of Polo-like kinase 4. *Science* 348, 1155–1160.
- Yalgin, C., Ebrahimi, S., Delandre, C., Yoong, L.F., Akimoto, S., Tran, H., Amikura, R., Spokony, R., Torben-Nielsen, B., White, K.P., et al. (2015). Centrosomin represses dendrite branching by orienting microtubule nucleation. *Nat. Neurosci.* 18, 1437–1445.
- Zhu, X., and Kaverina, I. (2013). Golgi as an MTOC: making microtubules for its own good. *Histochem. Cell Biol.* 140, 361–367.
- Zhu, X., Hu, R., Brissova, M., Stein, R.W., Powers, A.C., Gu, G., and Kaverina, I. (2015). Microtubules negatively regulate insulin secretion in pancreatic beta cells. *Dev. Cell* 34, 656–668.